Optimizing Imperceptibility and Robustness Using Selective DCT Coefficients for Image Copyright Protection

Majid Rahardi
Department of Informatics, Faculty of Computer Science, Universitas Amikom Yogyakarta, Sleman, 55283, Indonesia
majid@amikom.ac.id (corresponding author)

Afrig Aminuddin
Department of Information System, Faculty of Computer Science, Universitas Amikom Yogyakarta, Sleman, 55283, Indonesia
afrig@amikom.ac.id

Ferian Fauzi Abdulloh
Department of Informatics, Faculty of Computer Science, Universitas Amikom Yogyakarta, Sleman, 55283, Indonesia
ferian@amikom.ac.id

Nafiatun Sholihah
Department of Informatics, Postgraduate Program, Universitas Amikom Yogyakarta, Sleman, 55283, Indonesia
nafiatun@amikom.ac.id

Ferda Ernawan
Department of Computer Graphic and Multimedia, Faculty of Computing, Universiti Malaysia Pahang, Pekan, 26600, Malaysia
ferda@umpsa.edu.my

Received: 14 January 2025 | Revised: 4 March 2025 and 24 May 2025 | Accepted: 30 May 2025

 DOI: https://doi.org/10.48084/etasr.10241

ABSTRACT

This paper presents an invisible watermarking technique for image copyright protection based on the Discrete Cosine Transform (DCT). The proposed method balances imperceptibility and robustness against various image manipulations, such as JPEG compression, filtering, and noise attacks. By embedding the watermark into high-frequency DCT coefficients, the technique ensures minimal visual distortion while preserving watermark integrity. The experimental results demonstrate that the proposed method achieves high Peak Signal-to-Noise Ratio (PSNR) values, averaging 51.81 dB across multiple test images, and excellent structural similarity with an average Structural Similarity Index Measure (SSIM) of 0.9993. The proposed method also shows strong resilience to image tampering, with Normalized Cross-Correlation (NC) values of 0.7593 and low Bit Error Rate (BER) values of 0.1190 under various attack scenarios. These results highlight the method's effectiveness in protecting image copyright while maintaining computational efficiency.

Keywords-copyright protection; discrete cosine transform; image watermarking

I. INTRODUCTION

The rapid growth of digital technologies has transformed how information is created, shared, and distributed. With this transformation, protecting digital content such as images, audio, and video has become more challenging [1]. Unauthorized reproduction, distribution, and manipulation of digital media are increasingly common, posing serious threats

to intellectual property rights [2]. Digital watermarking has emerged as a vital solution for protecting digital assets, particularly images. Watermarking involves embedding a unique identifier (watermark) into the media content to establish ownership or authenticity. Digital watermarking techniques are generally classified into visible and invisible watermarking [3]. Visible watermarking is often applied to publicly shared images, incorporating a semi-transparent logo or text overlay to indicate ownership. Although effective for basic copyright protection, this method can compromise the visual appeal of the image. In contrast, invisible watermarking, which is the focus of this study, embeds information in a way that remains undetectable to the human eye [4]. This approach is particularly beneficial in professional copyright protection, as it preserves the original image quality while ensuring ownership verification.

In the realm of invisible watermarking, various methods have been developed to balance the need for robustness (the ability to withstand image manipulations such as compression, resizing, and noise) with imperceptibility (ensuring the embedded watermark does not distort the visual quality of the image) [5]. Techniques that operate in the frequency domain, such as those based on the Discrete Cosine Transform (DCT), have proven particularly effective. The DCT transforms an image from the spatial domain to the frequency domain, allowing watermarking algorithms to embed information into less noticeable parts of the image, such as high-frequency components, without significantly altering the image's appearance [6].

In addition to robustness and imperceptibility, computational efficiency is a key consideration in developing watermarking algorithms [7]. As digital watermarking systems become more integrated into real-time applications, such as content delivery platforms and image databases, ensuring these algorithms are fast and efficient without sacrificing performance is critical. Furthermore, resilience to common image attacks such as compression, rotation, scaling, and cropping remains a significant challenge in the field [8].

Several studies have proposed improvements to existing watermarking techniques to address these challenges. For example, algorithms leveraging multi-level transforms or optimization techniques such as Particle Swarm Optimization (PSO) have been explored to enhance the robustness of watermarking schemes [9]. Despite these advances, many proposed methods suffer from high computational complexity or are limited in their practical applicability, especially when balancing robustness against multiple types of image attacks and the need for real-time performance [10]. Given these challenges, there is a need for watermarking techniques that offer a more efficient, robust, and imperceptible solution [11]. A robust watermarking system should not only withstand a wide range of manipulations but also maintain the image's original quality, thus ensuring that the watermark remains hidden from the viewer while being detectable by watermark extraction algorithms.

Authors in [12] proposed a Quaternion Singular Value Decomposition (QSVD)-based watermarking scheme to enhance efficiency, robustness, and invisibility in digital watermarking. The method improved image quality and real-time performance using a structure-preserving QSVD algorithm, adaptive embedding, and coefficient pair selection via normalized cross-correlation. It incorporated logistic chaotic maps for security and QR codes for capacity. The scheme showed superior performance against image attacks but faced challenges with quaternion computational complexity and required further real-world validation.

Authors in [13] proposed a copyright protection scheme using extended visual cryptography and curvelet transform to create meaningful ownership shares. By applying discrete curvelet transform on RGB components and using Baker's map for scrambling, the scheme enhanced security and robustness against image processing attacks while maintaining good imperceptibility. Watermarks were retrieved via XOR-superimposition of the master and ownership shares. Despite its effectiveness, the method showed low robustness to cropping and impulse noise, and it could benefit from further optimization of its computational complexity.

Authors in [14] proposed a blind dual watermarking scheme embedding a robust copyright protection watermark and a fragile authentication watermark. The robust watermark used Discrete Wavelet Transform (DWT), Human Visual System (HVS), and Singular Value Decomposition (SVD) domains, optimized by PSO for balance, whereas the fragile watermark manipulated RGB diagonal singular values to verify authenticity without reference images. The method demonstrated high robustness, imperceptibility, and tamper detection, outperforming 13 other schemes. However, it faced slight visual distortion to enhance capacity, as well as increased computational complexity due to the multiple transforms and optimizations involved.

Authors in [15] proposed a PSO and Kernel Elastic Least Squares (KELM)-based watermarking technique for multi-spectral image copyright protection. The method selected non-overlapping blocks based on texture, applied DCT, and used KELM to embed watermark bits, with PSO optimizing scaling factors. It showed high imperceptibility and robustness against various attacks, which were evaluated using Peak Signal-to-Noise Ratio (PSNR), Bit Error Rate (BER), and Normalized Cross-Correlation (NC) metrics. However, the method faced significant computational overhead from PSO optimization and lacked resistance to rotational attacks, requiring further enhancement.

Authors in [16] proposed a wavelet-packet-based watermarking technique for color image copyright protection. Applying wavelet-packet transforms to RGB layers and updating conjoint core trees ensured high imperceptibility and robustness against compression, filtering, noise, and manipulation attacks. It demonstrated superior performance to existing methods and had low computational cost, making it practical for real-world use. However, the technique was not evaluated for authentication or ownership verification, and it was tested on a limited dataset, leaving its broader effectiveness uncertain.

Authors in [17] introduced a robust zero-watermarking method for grayscale image copyright protection using

histogram features and the Sine Cosine Algorithm (SCA). A secret binary sequence from a user-selected Region of Interest (ROI) was used for validation, and SCA detected the ROI in attacked images. The method demonstrated high resistance to complex attacks like cropping and translation, maintaining efficiency and image integrity. However, the method was vulnerable to geometric attacks on large images and required subdividing them into blocks. It also relied on user-selected ROIs, limiting full automation.

Existing digital watermarking techniques struggle to balance computational efficiency, robustness against attacks, and practical applicability. Most methods excel in specific areas but face limitations in scalability, resistance to combined attacks, and real-world usability. To solve these issues, this paper introduces a novel DCT-based invisible watermarking technique achieving high imperceptibility (PSNR: 51.81 dB, Structural Similarity Index Measure (SSIM): 0.9993) and robustness against JPEG compression, filtering, and noise. Its computational efficiency enables real-time applications, outperforming existing methods in image quality and robustness, offering a practical solution for copyright protection.

II. PROPOSED METHOD

This chapter presents the watermark embedding and extraction processes based on the DCT for copyright protection. The evaluation metrics for image quality and watermark robustness are also discussed, using PSNR and SSIM for image quality, whereas NC and BER are used for watermark integrity after tampering. The diagram of the proposed method is shown in Figure 1.

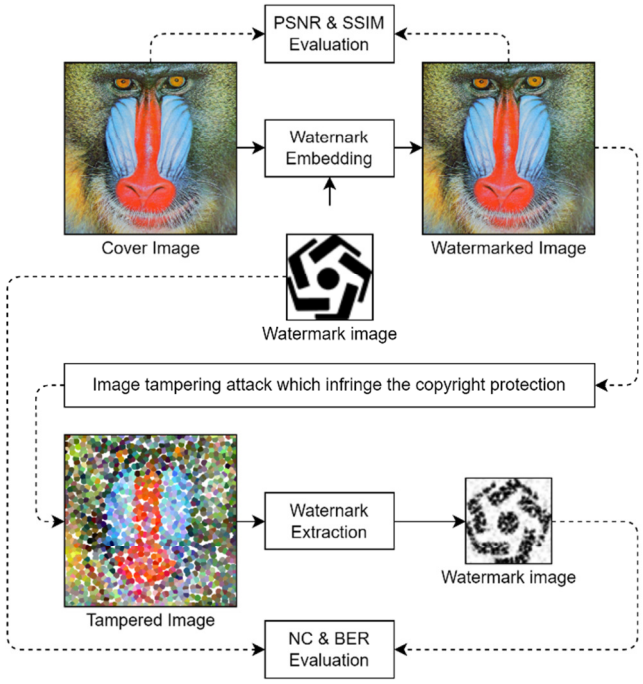

Fig. 1. The diagram of the proposed method and the performance evaluation techniques.

A. Watermark Embedding

The watermark embedding process begins with the cover image and embedding the watermark into the DCT coefficients of the cover image. The detailed steps are as follows:

1. Input image parsing and resizing: The cover image is loaded and resized to ensure it is divisible by the block size (8×8). If the image's dimensions are not divisible by 8, the image is resized using nearest-neighbor interpolation. This ensures that the entire image can be processed in non-overlapping blocks, which is essential for applying DCT-based embedding.
2. Watermark preparation: The watermark is binarized and resized to match the image's dimensions in blocks. The watermark is replicated across each channel (if the image is in color) to ensure uniform embedding across the entire image. The watermark is also scrambled using a Pseudo-Random Number Generator (PRNG), which helps secure the watermark data.
3. Block-wise DCT transformation: The resized image is divided into non-overlapping 8×8 blocks. For each block, the DCT is applied. DCT transforms the image from the spatial domain to the frequency domain, where watermark embedding occurs in the frequency coefficients.

$$\mathrm{DCT}(u,v) = \frac{1}{4}\sum_{x=0}^{7}\sum_{y=0}^{7} f(x,y)\cos\left[\frac{(2x+1)u\pi}{16}\right]\cdot \cos\left[\frac{(2y+1)v\pi}{16}\right] \quad (1)$$

where $f(x,y)$ is the pixel intensity in the spatial domain, and $\mathrm{DCT(u,v)}$ represents the transformed frequency domain.

4. Watermark embedding into DCT coefficients: Selected DCT coefficients are modified to embed the watermark as visualized in Figure 2. Specific low-frequency coefficients are chosen for each channel to insert the watermark bits. The embedding follows:

$$\mathrm{DCT}'(u,v) = \left\lfloor \frac{\mathrm{DCT}(u,v)}{scale} \right\rfloor \times scale + \frac{wm \times scale}{2} \quad (2)$$

where *scale* controls the strength of the watermark embedding.

5. Inverse DCT transformation: After embedding the watermark into the selected coefficients, the Inverse DCT (IDCT) is applied to each block to transform it back into the spatial domain. The result is the watermarked image block. This process is repeated for all blocks of the image.
6. Final watermarked image: The watermarked blocks are combined to form the final watermarked image, which is saved for further use. The embedding is done to maintain high fidelity with the original image, ensuring imperceptibility.

The choice of DCT coefficients for watermark embedding is a crucial factor that directly impacts both the imperceptibility and robustness of the watermarking scheme. In our previous

work [6], we utilized a fixed set of mid-frequency DCT coefficients for embedding, which provided a reasonable balance between visual quality and resistance to common image processing attacks. However, further analysis and experimentation revealed that a more selective approach—targeting specific high-frequency DCT coefficients—can yield superior results.

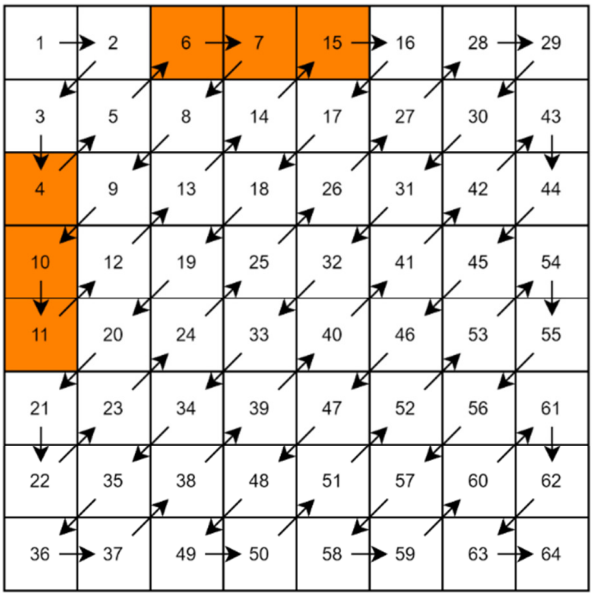

Fig. 2. Selected DCT coefficients embedding location.

The rationale behind this selection is twofold. First, high-frequency DCT coefficients are less perceptible to the human visual system. Consequently, modifications in these regions are less likely to introduce visible artifacts, thereby preserving the image's visual quality (as evidenced by the higher PSNR and SSIM values in our results). Secondly, by carefully selecting the high-frequency coefficients be used—based on empirical testing of their resilience to attacks such as JPEG compression, filtering, and noise—we ensure that the embedded watermark remains robust and recoverable even after such manipulations.

Additionally, in this work, we enhance security by scrambling the watermark using a PRNG before embedding. This not only distributes the watermark bits more uniformly across the image but also makes unauthorized detection or removal of the watermark significantly more difficult.

Our experimental results confirm that this selective and randomized embedding strategy leads to improved imperceptibility and robustness compared to both our previous method and other state-of-the-art techniques. This finding underscores the importance of a systematic and empirically driven approach to DCT coefficient selection in the design of practical and secure image watermarking systems.

B. Watermark Extraction

The watermark extraction process is the inverse of the embedding, retrieving the watermark from the DCT coefficients of the possibly tampered image. The steps are detailed as follows:

1. Loading and resizing the tampered image: The tampered image is loaded and resized to match the original image's dimensions. This ensures compatibility during the block-wise DCT processing.
2. Block-wise DCT transformation: The tampered image is divided into non-overlapping 8×8 blocks, and DCT is applied to each block. This converts the image into its frequency components, from which the watermark bits can be extracted.
3. Watermark extraction from DCT coefficients: The previously modified DCT coefficients are read from each block to extract the embedded watermark bits. The extraction is based on checking the modified values of the coefficients:

$$wm = \begin{cases} 1, & \text{if } \frac{scale}{4} < coef < \frac{3 \cdot scale}{4} \\ 0, & \text{otherwise} \end{cases} \quad (3)$$

$$coef = \text{mod}(\text{DCT}(u, v), scale) \quad (4)$$

The extracted watermark bits are aggregated to form the complete watermark.

4. Watermark reconstruction: The extracted watermark is reconstructed and compared with the original watermark to assess the robustness of the proposed method.

C. Evaluation Metrics

The imperceptibility of the proposed method is evaluated by comparing the cover image and the watermarked image using PSNR and SSIM. The robustness of the proposed method is evaluated by comparing the original watermark with the extracted watermark using NC and BER. PSNR is used to measure the imperceptibility of the watermark by comparing the cover image with the watermarked image. It is defined as:

$$\text{PSNR} = 10 \cdot \log_{10}\left(\frac{MAX^2}{MSE}\right) \quad (5)$$

where MAX is the maximum possible pixel value, and MSE is the mean squared error between the cover and watermarked images. SSIM measures the perceptual similarity between the original cover image and the watermarked image. The SSIM is defined as:

$$\text{SSIM}(x, y) = \frac{(2\mu_x\mu_y + C_1)(2\sigma_{xy} + C_2)}{(\mu_x^2 + \mu_y^2 + C_1)(\sigma_x^2 + \sigma_y^2 + C_2)} \quad (6)$$

where μ_x and μ_y are the means of the original and watermarked images, σ_x^2 and σ_y^2 are the variances, σ_{xy} is the covariance and C_1, C_2 are constants for stability. NC compares the original and extracted watermarks. It is defined as:

$$\text{NC} = \frac{\sum_{i,j} W(i,j) \cdot \widehat{W}(i,j)}{\sqrt{\sum_{i,j} W(i,j)^2} \cdot \sqrt{\sum_{i,j} \widehat{W}(i,j)^2}} \quad (7)$$

where $W(i,j)$ represents the original watermark and $\widehat{W}(i,j)$ represents the extracted watermark. BER measures the error

rate between the original and extracted watermarks after the image has undergone tampering. It is defined as:

$$\text{BER} = \frac{1}{n}\sum_{i=1}^{n}\left|W(i) - \widehat{W}(i)\right| \quad (8)$$

where n is the total number of watermark bits, $W(i)$ and $\widehat{W}(i)$ are the original and extracted watermark bits, respectively.

III. RESULTS AND DISCUSSION

This chapter presents the results of the experimental evaluation of the proposed invisible watermarking technique based on DCT. The system's performance is analyzed in terms of imperceptibility, robustness, and computational efficiency. Key evaluation metrics include PSNR, SSIM, NC, and BER.

The experiments use eight color images from the USC-SIPI dataset [18], each with a resolution of 512×512 pixels. These images are used as cover images to embed the invisible watermark. The watermark is a binary image embedded using the proposed block-wise DCT-based embedding process. All experiments are performed on a PC with AMD Ryzen 5 4500U processor and MATLAB R2021a.

A. Watermarked Image Quality

After embedding the watermark using the DCT-based technique described in Chapter II, the quality of the watermarked images is assessed using PSNR and SSIM. PSNR measures the distortion between the original and watermarked images, where higher PSNR values indicate lower distortion. SSIM is used to measure the perceptual similarity between the two images. Table I presents a comparative analysis of the watermarking performance between our previous work in [6] and the proposed method based on three key metrics: PSNR, SSIM, and processing time.

TABLE I. COMPARISON OF THE WATERMARKED IMAGE QUALITY WITH PREVIOUS WORK

Image	[6]			Proposed method		
	PSNR (dB)	SSIM	Time (s)	PSNR (dB)	SSIM	Time (s)
Airplane	50.51	0.9963	0.6562	51.79	0.9973	0.7031
Baboon	49.97	0.9996	0.6875	51.53	0.9997	0.7031
House	50.51	0.9989	0.8750	51.86	0.9992	0.7344
Lena	50.34	0.9997	0.7188	51.71	0.9998	0.6406
Pepper	50.31	0.9997	0.6250	51.72	0.9998	0.6406
Sailboat	50.19	0.9993	0.6250	51.69	0.9995	0.6250
Splash	50.83	0.9995	0.6094	51.94	0.9996	0.7188
Tiffany	50.93	0.9996	0.7344	52.25	0.9997	0.7656
Average	50.45	0.9991	0.6914	51.81	0.9993	0.6914

As demonstrated in Table I, the proposed method consistently achieves higher PSNR values across all test images, with an average PSNR of 51.81 dB compared to 50.45 dB in [6], indicating better preservation of image quality. Similarly, the SSIM values show a slight improvement, suggesting that the proposed method maintains structural fidelity more effectively. Although the processing time varies slightly across different images, the average execution time remains the same at 0.6914 s, demonstrating that the proposed method enhances image quality without increasing computational overhead. These results highlight the effectiveness of the proposed watermarking technique in improving imperceptibility while maintaining efficiency. The cover, delta, and watermarked images corresponding to the method in [6] are presented in Figure 3, whereas those produced by the proposed method are shown in Figure 4. Figure 3 shows that the previous method in [6] reveals the watermark artifact in the delta image. This leads to predictable watermark content which could benefit the attacker. The attacker could remove or replace the watermark data with a new watermark image. On the other hand, the proposed method randomizes the watermark data using a PRNG to ensure the safety of the watermark data.

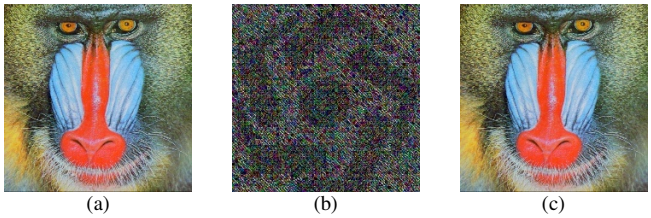

(a) (b) (c)

Fig. 3. Watermark embedding of the Baboon image for the method in [6]: (a) cover image, (b) delta image, (c) watermarked image.

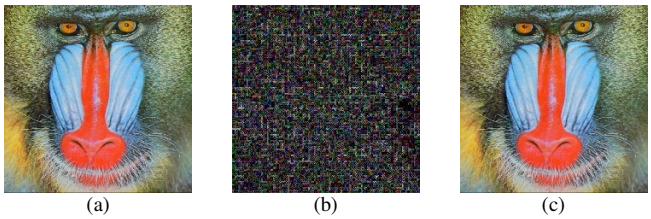

(a) (b) (c)

Fig. 4. Watermark embedding of the Baboon image for the proposed method: (a) cover image, (b) delta image, (c) watermarked image.

Table II presents a comparative analysis of the performance of the proposed watermarking method with three existing approaches. The analysis is conducted in terms of PSNR, SSIM, and processing time. The proposed method achieves the highest PSNR (51.81 dB), indicating its superiority in preserving image quality compared to the methods described in [19] (48.82 dB), [20] (47.65 dB), and [6] (50.45 dB). Additionally, the SSIM value (0.9993) of the proposed method (0.9993) exhibits a marginal increase over the value reported in [6] (0.9991) and a substantial improvement compared to the values in [19] (0.9925) and [20] (0.9953), demonstrating better structural integrity retention. With regard to processing time, the proposed method (0.6914 s) is equivalent to [6] and is notably more efficient than [20] (1.5734 s). These results indicate that the proposed method outperforms previous approaches by achieving better imperceptibility and efficiency while maintaining competitive processing speed.

TABLE II. WATERMARKED IMAGE COMPARISON BETWEEN VARIOUS METHODS

Method	PSNR (dB)	SSIM	Time (s)
[19]	48.82	0.9925	0.6877
[20]	47.65	0.9953	1.5734
[6]	50.45	0.9991	0.6914
Proposed	51.81	0.9993	0.6914

B. Robustness of Watermark Extraction

The robustness of the watermark extraction process is tested by applying various attacks to the watermarked images, such as JPEG compression, Gaussian filter, median filter, mosaic filter, ripple mask, salt and pepper, sharpen, and unsharp filter. The watermark is extracted after each attack, and the quality of the extracted watermark is evaluated using NC and BER. Table III presents a comparative evaluation of robustness against various tampering attacks between our previous work in [6] and the proposed method. The comparison is based on three key metrics: NC, BER, and processing time.

TABLE III. COMPARISON OF THE ROBUSTNESS AGAINST TAMPERING ATTACKS

Tampering attack	[6]			Proposed method		
	NC	BER	Time (s)	NC	BER	Time (s)
JPEG 90%	0.7445	0.1344	0.3574	0.7463	0.1255	0.3125
JPEG 70%	0.7395	0.1372	0.3633	0.7465	0.1254	0.3223
JPEG 50%	0.7395	0.1414	0.3438	0.7456	0.1258	0.3223
Gaussian filter	0.7386	0.1386	0.3535	0.7451	0.1261	0.3360
Median filter	0.7573	0.1225	0.3223	0.7553	0.1209	0.3008
Mosaic filter	0.7509	0.1279	0.3399	0.7588	0.1190	0.3028
Ripple mask	0.7455	0.1268	0.3281	0.7428	0.1272	0.3125
Salt and pepper	0.8484	0.0750	0.3340	0.8438	0.0771	0.3223
Sharpen	0.7735	0.1132	0.3516	0.7552	0.1212	0.3106
Unsharp filter	0.7434	0.1273	0.3301	0.7539	0.1219	0.3184
Average	0.7581	0.1244	0.3424	0.7593	0.1190	0.3160

As demonstrated in Table III, the proposed method consistently achieves higher NC values and lower BER across most attacks, indicating improved robustness in watermark recovery. Notably, the proposed method exhibits significant improvements against JPEG compression, median filtering, and mosaic filtering, with an average NC of 0.7593 compared to 0.7581 in [6], and a lower BER of 0.1190 compared to 0.1244 in [6]. Additionally, the proposed method exhibits faster execution times, averaging 0.3160 s, compared to 0.3424 s in [6], showcasing its computational efficiency. While minor trade-offs are observed in certain cases, such as the ripple mask and sharpening attack, the overall results highlight the effectiveness of the proposed technique in enhancing watermark robustness while maintaining efficiency.

IV. CONCLUSION

This paper proposed an invisible watermarking technique based on Discrete Cosine Transform (DCT) that optimizes the trade-off between imperceptibility and robustness for image copyright protection. By selectively embedding the watermark into high-frequency DCT coefficients, our method minimizes visual distortion while maintaining strong resistance against various attacks, including JPEG compression, filtering, and noise addition. The experimental results demonstrate the effectiveness of the proposed approach, achieving an average Peak Signal-to-Noise Ratio (PSNR) of 51.81 dB, a Structural Similarity Index Measure (SSIM) of 0.9993, and strong watermark recovery with a Normalized Cross-Correlation (NC) of 0.7593 and a low Bit Error Rate (BER) of 0.1190. Compared to previous DCT-based methods, our approach improves imperceptibility and robustness while maintaining computational efficiency, making it suitable for real-world applications. The novelty of our approach lies in enhancing traditional DCT-based watermarking techniques by integrating selective coefficient embedding with Pseudo-Random Number Generator (PRNG)-based watermark randomization. Unlike conventional methods that embed the watermark in predefined frequency bands, our technique randomizes watermark data before embedding, increasing security and resilience against unauthorized removal or tampering. This approach ensures higher watermark integrity even under common attacks, making the method more secure for copyright protection. Future research can explore adaptive embedding strategies for dynamic watermarking applications.

ACKNOWLEDGMENT

This research is supported by the Ministry of Higher Education of Indonesia under Fundamental Research Grant No. 107/E5/PG.02.00.PL/2024 and 0609.20/LL5-INT/AL.04/2024.

REFERENCES

[1] A. Mohanarathinam, S. Kamalraj, G. K. D. Prasanna Venkatesan, R. V. Ravi, and C. S. Manikandababu, "Digital watermarking techniques for image security: a review," *Journal of Ambient Intelligence and Humanized Computing*, vol. 11, no. 8, pp. 3221–3229, Aug. 2020, https://doi.org/10.1007/s12652-019-01500-1.

[2] L. Rakhmawati, W. Wirawan, S. Suwadi, C. Delpha, and P. Duhamel, "Blind robust image watermarking based on adaptive embedding strength and distribution of quantified coefficients," *Expert Systems with Applications*, vol. 187, Jan. 2022, Art. no. 115906, https://doi.org/10.1016/j.eswa.2021.115906.

[3] I. J. Cox, M. L. Miller, J. A. Bloom, J. Fridrich, and T. Kalker, Eds., *Preface to the Second Edition*, 2nd ed. San Francisco, CA, USA: Morgan Kaufmann, 2008.

[4] R. Zhu and X. Wang, "Efficient Digital Watermarking in DCT Domain," in *2009 International Forum on Information Technology and Applications*, Chengdu, China, 2009, pp. 587–590, https://doi.org/10.1109/IFITA.2009.88.

[5] M. Begum and M. S. Uddin, "Digital Image Watermarking Techniques: A Review," *Information*, vol. 11, no. 2, Feb. 2020, Art. no. 110, https://doi.org/10.3390/info11020110.

[6] M. Rahardi, F. F. Abdulloh, and W. S. Putra, "A Blind Robust Image Watermarking on Selected DCT Coefficients for Copyright Protection," *International Journal of Advanced Computer Science and Applications*, vol. 13, no. 7, pp. 719–726, Jul. 2022, https://doi.org/10.14569/IJACSA.2022.0130785.

[7] A. F. Qasim, F. Meziane, and R. Aspin, "Digital watermarking: Applicability for developing trust in medical imaging workflows state of the art review," *Computer Science Review*, vol. 27, pp. 45–60, Feb. 2018, https://doi.org/10.1016/j.cosrev.2017.11.003.

[8] Y. Luo, X. Tan, and Z. Cai, "Robust Deep Image Watermarking: A Survey," *Computers, Materials and Continua*, vol. 81, no. 1, pp. 133–160, Oct. 2024, https://doi.org/10.32604/cmc.2024.055150.

[9] F. Thakkar and V. K. Srivastava, "An adaptive, secure and imperceptive image watermarking using swarm intelligence, Arnold transform, SVD and DWT," *Multimedia Tools and Applications*, vol. 80, no. 8, pp. 12275–12292, Mar. 2021, https://doi.org/10.1007/s11042-020-10220-0.

[10] A. Munshi, "Randomly-based Stepwise Multi-Level Distributed Medical Image Steganography," *Engineering, Technology & Applied Science Research*, vol. 13, no. 3, pp. 10922–10930, Jun. 2023, https://doi.org/10.48084/etasr.5935.

[11] Laxmanika and P. K. Singh, "Robust and imperceptible image watermarking technique based on SVD, DCT, BEMD and PSO in wavelet domain," *Multimedia Tools and Applications*, vol. 81, no. 16, pp. 22001–22026, Jul. 2022, https://doi.org/10.1007/s11042-021-11246-8.

[12] Y. Chen, Z. Jia, Y. Peng, and Y. Peng, "Efficient Robust Watermarking Based on Structure-Preserving Quaternion Singular Value Decomposition," *IEEE Transactions on Image Processing*, vol. 32, pp. 3964–3979, 2023, https://doi.org/10.1109/TIP.2023.3293773.

[13] S. Kukreja, G. Kasana, and S. S. Kasana, "Copyright protection scheme for color images using extended visual cryptography," *Computers & Electrical Engineering*, vol. 91, no. 2, May 2021, Art. no. 106931, https://doi.org/10.1016/j.compeleceng.2020.106931.

[14] S. B. B. Ahmadi, G. Zhang, M. Rabbani, L. Boukela, and H. Jelodar, "An intelligent and blind dual color image watermarking for authentication and copyright protection," *Applied Intelligence*, vol. 51, no. 3, pp. 1701–1732, Mar. 2021, https://doi.org/10.1007/s10489-020-01903-0.

[15] V. Sisaudia and V. P. Vishwakarma, "Copyright protection using KELM-PSO based multi-spectral image watermarking in DCT domain with local texture information based selection," *Multimedia Tools and Applications*, vol. 80, no. 6, pp. 8667–8688, Mar. 2021, https://doi.org/10.1007/s11042-020-10028-y.

[16] H. M. Al-Otum, "Wavelet packets-based watermarking with preserved high color image quality and enhanced robustness for copyright protection applications," *Multimedia Tools and Applications*, vol. 78, no. 2, pp. 2199–2225, Jan. 2019, https://doi.org/10.1007/s11042-018-6328-3.

[17] A. Daoui, H. Karmouni, M. Sayyouri, Q. Hassan, M. Maaroufi, and B. Alami, "New Robust Method for Image Copyright Protection Using Histogram Features and Sine Cosine Algorithm," *Expert Systems with Applications*, vol. 177, no. 3, Apr. 2021, Art. no. 114978, https://doi.org/10.1016/j.eswa.2021.114978.

[18] "The USC-SIPI Image Database." Kaggle. [Online]. Available: https://www.kaggle.com/datasets/luffyluffyluffy/the-uscsipi-image-database.

[19] M. Yousefi Valandar, M. Jafari Barani, and P. Ayubi, "A blind and robust color images watermarking method based on block transform and secured by modified 3-dimensional Hénon map," *Soft Computing*, vol. 24, no. 2, pp. 771–794, Jan. 2020, https://doi.org/10.1007/s00500-019-04524-z.

[20] R. Thanki, A. Kothari, and D. Trivedi, "Hybrid and blind watermarking scheme in DCuT – RDWT domain," *Journal of Information Security and Applications*, vol. 46, no. C, pp. 231–249, Jun. 2019, https://doi.org/10.1016/j.jisa.2019.03.017.